

Propagative Mode in a Lattice-Grain CA: Time Evolution and Timestep Synchronization

Dominique Désérable

INSA – Institut National des Sciences Appliquées,
Laboratoire de Génie Civil & Génie Mécanique,
20 Avenue des Buttes de Coësmes, 35043 Rennes, France
deserable@insa-rennes.fr
<http://www.insa-rennes.fr>

Abstract. The void propagation defines a long-range interaction in granular matter. We detail a logic scheme simulating the propagation and implemented in a $2d$ cellular automata applied to granular flow. The CA belongs to the family of “lattice-grain” automata (LGrA) with one particle per cell. We focus first on the influence of inertia, or “memory effect”, on the flow patterns. The propagative mode is presented afterwards: it implies that transition and timestep must be considered at two different time scales. Although a CA is usually driven by local, nearest-neighbor communications, it follows here that the timestep termination must be detected at each transition, that involves a perpetual and global communication within the network to synchronize the timestep. An all-to-all “systolic gossiping” underlies the framework of this void propagation model.

Keywords: lattice-grain (cellular) automata (LGrA), void propagation, memory effect, time evolution, timestep synchronization, systolic gossiping.

1 Introduction

Cellular automata may capture the essence of physical phenomena resulting from elementary factors and make a suitable and powerful tool to catch the influence of the microscopic scale onto the macroscopic behavior of complex systems [1]. Known as “lattice-gas” (cellular) automata (LGA) in hydrodynamics, they are an extreme simplification of molecular dynamics and have been widely developed over the last forty years. Concerning granular media, there was a number of attempts which in turn make a relative simplification of granular dynamics and which are often known as “lattice-grain” (cellular) automata (LGrA); they have yielded some interesting results especially for hopper flows, flows around obstacles, segregation or stratification phenomena during free surface multiphase flows or the formation of density waves in channel flows [2,3,4,5,6,7,8]. A state of the art for lattice-grain models is given in [9] with references therein.

We focus here on a specific feature of our LGrA [10,11] concerning its capability of handling long-range interactions resulting from the phenomenon of void

propagation in a granular assembly. The time evolution is governed by a “request-exchange” synchronous mode which simulates a two-stage interaction-advection process. The transition rule follows a simple logic including three physical components: an external field, a set of kinematical exclusion rules and an inertial effect. Our model is inspired by the first discrete, analytic model of Litwiniszyn-Müllins [12,13] dealing with granular flow under gravity and including a “memory” effect of inertia.

Section 2 recalls our LGrA logic that defines how the time evolution is driven by the local interaction law acting on the hexavalent lattice. The inertial, memory effect is illustrated through a case study in Section 3. Section 4 describes the logic of the propagative mode acting on the void. After a short reference to the works upon the intensive communication protocols in coarse-grain and fine-grain massively parallel architectures, Section 5 explains how the timestep synchronization scheme induced by the long-range propagative logic is carried out by means of a perpetual “systolic gossiping”. We conclude in Section 6 by asking the question of the consistency of our model with the physical time as an open problem.

2 LGrA Logic

2.1 Topology and Local Interaction Law

The LGrA is constructed on the 6-*valent* grid. This $2d$ topology offers the greatest number of symmetries for a regular lattice: herein it maximizes the number of *degrees of freedom* (or directions) for a displacement as well as the upper bound of the *coordination number* (the number of contacts of a particle with its vicinity). The concise notation “ ν df” ($0 \leq \nu \leq 6$) will be used for a law with ν degrees of freedom. Each site is connected to its six nearest neighbors denoted NE, N, NW, SW, S, SE . The order N_s stands for the number of sites of the network. Since the graph is regular with degree 6, the number of links connecting a pair of adjacent sites is clearly $3N_s$.

The *space occupancy* principle allows one and only one particle per site, whether it is a solid, liquid or gaseous one, the term “particle” being a purely formal denotation. Multiphase flows are considered, where a phase ϕ_i , indexed in the set $N_\phi = \{1, 2, \dots, n_\phi\}$ for a system of n_ϕ phases, denotes a set of particles provided with identical properties.

The *interaction-advection* process is performed by a two-stage transition according to an original “request-exchange” mechanism. In the *request* stage, each cell autonomously performs a computation composed of a precalculation followed by a random choice. The result is a *potential* direction of displacement which becomes the direction of request. In the *exchange* stage, a test is performed for each link of the network in order to detect whether an agreement has been reached between the potential directions yielded by both adjacent sites (*interaction*). In this case, a cell-to-cell exchange is performed (*advection*).

The behavior of a *phase* in a multiphase system is defined by three “physical” components: an external field, a set of exclusion rules and an inertial effect. It

should be pointed out that it is not so much the autonomous behavior law of a given phase that must be taken into account but the *interaction* law with its local neighborhood: a phase component is meaningful, only when embedded into the interaction law.

2.2 Time Evolution Equations and Transition Rule

A set $K = (0, 1, 2, 3, 4, 5)$ is assigned to the six directions NE, N, NW, SW, S, SE . For a given timestep, a cell contains a particle of phase ϕ_i ($i \in N_\phi$) characterized by the three following components:

- the action of an *external field*, depicted by a “ ν df” law with a 6-fold vector

$$W_i = (w_i^{(k)})_{k \in K} \quad (1)$$

where weights $w_i^{(k)}$ are non-negative integers and ν is the number of positive weights.

- the action of *exclusion rules*, precluding some direction or other depending on the state of the local vicinity and acting according to a *mode* from which the exclusion will be applied before (*pre-exclusion*) or after (*post-exclusion*) the request. This action is depicted by the 6-fold binary vector

$$\tilde{\mathcal{E}}_i = (\tilde{\varepsilon}_i^{(k)})_{k \in K} : \tilde{\varepsilon}_i^{(k)} = r_i \varepsilon_i^{(k)} + (1 - r_i) \quad (2)$$

where $\varepsilon_i^{(k)} = 0$ (or 1) whenever the site in direction k is excluded (or not) and $r_i = 1$ (resp. 0) for a pre (resp. post) mode assigned to the phase. In the sequel, a pre-exclusion will always be assumed, that simplifies (2) into

$$\mathcal{E}_i = (\varepsilon_i^{(k)})_{k \in K} . \quad (3)$$

- the action of *inertia*, or “memory” effect, depicted by the 6-fold vector

$$\mathcal{M}_i = (\mu_i^{(k)})_{k \in K} \quad (4)$$

where $\mu_i^{(k)} = c_i$ if k was the displacement direction at the previous timestep and $\mu_i^{(k)} = 1$ otherwise. Coefficient c_i takes on positive integer values and $c_i = 1$ means no inertia for the phase.

Prior to computing a request, a precalculation yields the corrected distribution

$$W_i^* = (w_i^{*(k)})_{k \in K} : w_i^{*(k)} = \mu_i^{(k)} \varepsilon_i^{(k)} w_i^{(k)} \quad (5)$$

and the probability of sending a request in direction k is then given by

$$p_i^{*(k)} = \frac{w_i^{*(k)}}{\sum_K w_i^{*(k)}} \quad (6)$$

on condition that the sum of the corrected distribution be positive ($p_i^{*(k)} = 0$ otherwise). Direction k is selected at random by a pseudorandom sequence generated from a user-defined seed.

Let $(p_j^{*(k)})_{k \in K}$ be now the distribution of probabilities of the neighboring particle of phase ϕ_j in direction k and let X_k be the representative event of a displacement in direction k for the current particle. The probability of this event is finally

$$P(X_k) = p_i^{*(k)} p_j^{*(k+3 \bmod 6)} \quad (7)$$

according to the exchange protocol.

For brevity's sake, the reader is referred to [10,11] for a more detailed description of our LGrA logic.

3 Inertia and Memory Effect

Modeling inertia consists in saving the *memory* of the particle's displacement direction at the previous timestep, to reintroduce it with a user-defined weight into the new weighted distribution for the current timestep. An *inertial* coefficient c_i , which takes on a positive integer value, is assigned to each phase ϕ_i and $c_i = 1$ means no inertial effect for this phase.

3.1 A Case Study

The memory effect will be illustrated through a simple granular system simulating a silo emptying process. A silo is a container provided with an outlet through which bulk grain falls down. A two-phase system $N_\phi = \{1, 2\}$ is considered, where ϕ_1 denotes the “grain” phase and ϕ_2 the “void” phase. Let us recall the set $K = (0, 1, 2, 3, 4, 5)$ assigned to the six directions NE, N, NW, SW, S, SE . Regarding the gravity axis, we adopt two scenarios:

- a “2df–2df” law (shortly denoted “2df”) with $W_1 = (1, 0, 0, 0, 0, 1)$, $W_2 = (0, 0, 1, 1, 0, 0)$ where the pattern NE – SE means “downwards”, the sense of the main axis being $W \rightarrow E$;
- a “3df–3df” law (shortly denoted “3df”) with $W_1 = (0, 0, 0, 1, 1, 1)$, $W_2 = (1, 1, 1, 0, 0, 0)$ where the pattern SW – S – SE means “downwards”, the sense of the main axis being $N \rightarrow S$.

A “frontal” exclusion rule R_1 is assigned to ϕ_1 and ϕ_2 : this rule prohibits two particles with the same phase to exchange. That is, neither a grain-grain nor a void-void exchange may occur.

The size of the container is defined by its height $H = 101$, its width $L = 57$, giving a volume V_0 of 5707 or 5729 cells, respectively for the “2df” or the “3df” law; the negligible deviation (of 0.4%) results from a side-effect of the lattice. The container is flat-bottomed and has no hopper, namely, its shape is rectangular. The outlet, centered in the bottom, has a diameter $D = 7$ cells. The cells in the outlet play a special role of “source” cells generating a void when a grain

exits. The instantaneous “flow rate” is defined as the number of exiting grains (or generated voids) per timestep. Initially, the silo is fully filled with grains. The “porosity”, in this context, is defined from the ratio void/grain, namely zero at initial state. A qualitative observation of the flow is made easier by zoning the material into horizontal colored layers.

3.2 Influence of Inertia on Flow Patterns

Figure 1 highlights the action of inertia for the “2df” law under rule R_1 after $T = 600$ timesteps. In (a), no inertia is applied and a “funnel flow” is observed where the upper layers fall down first. In (b), an inertial coefficient $c_2 = 10$ is applied to the void phase and a “mass flow” is observed with a strong dissymmetry in the emptying process. The dissimilarity between both patterns results only from two distinct values assigned to the seed of the pseudorandom sequence, that reveals here a sensitive dependence on initial conditions. A hopper-shaped pattern between two shear bands separates the dynamic flow from a static “dead zone”, with an angle of stability of 60° induced by the “2df” law. Moreover, the chaotic free surface is induced by the flow above the outlet, which periodically alternate from one shear band to the other. This kind of flow pattern was experimentally observed [14]. A *propagative* effect acting on the voids upgoing from the outlet appears on both sides of the hopper, though with an abnormally high porosity.

The action of inertia for the “3df” law is displayed in Fig. 2 at state $T = 1000$. In (a), no inertia is applied and a (last-in first-out) “funnel flow” is again observed but with a reduction of the funnel’s depth. In (b-c), an inertial coefficient

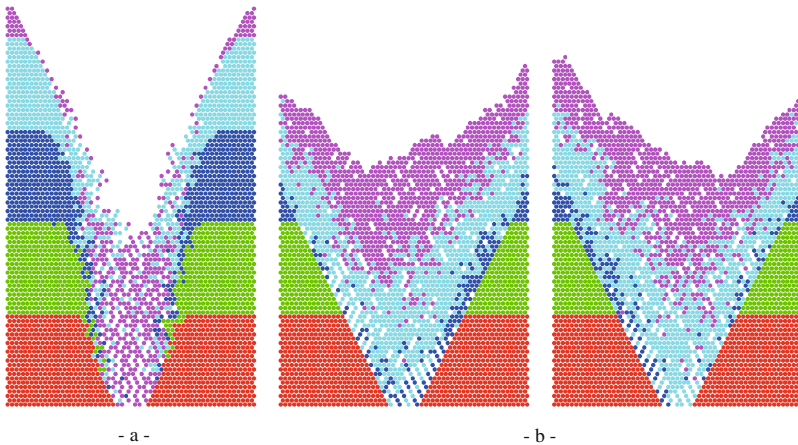


Fig. 1. “2df” law with rule R_1 governing ϕ_1 and ϕ_2 . States at $T = 600$ (a) without inertial action (b) with inertial coefficients $c_1 = 1$ and $c_2 = 10$ and two distinct values of the seed of the pseudorandom sequence

$c_2 = 10$ is applied to the void and a (first-in first-out) “mass flow” is again observed but with a non-chaotic behavior and only weak instabilities appearing on the free surface. A hopper-shaped pattern between two shear bands still separates the dynamic flow from a static dead zone, but with an angle of stability of 30° induced by the “3df” law. As a consequence, the void phase is distributed throughout the entire bulk, possibly with a porosity ratio higher than the normal average, compared with which could be experimentally observed. Besides, while a same value $c_1 = c_2$ is assigned to the grain phase in (b), no significant behavioral discrepancy can be observed. Therefore, it should be pointed out that the impact of a “memory” assigned to the void is significant whereas a “memory” assigned to the grain is irrelevant in a dense packing.

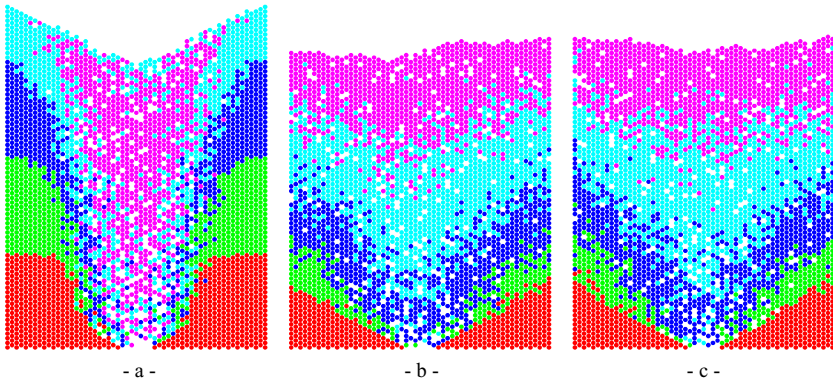


Fig. 2. “3df” law with rule R_1 governing ϕ_1 and ϕ_2 . States at $T = 1000$ (a) without inertial action (b) with inertial coefficients $c_1 = c_2 = 10$ (c) with $c_1 = 1$, $c_2 = 10$.

From the above observations, it may be asked what *physical* meaning could be attributed to the artifact giving inertia to the *void*. Whenever a high value is assigned to the “memory” of the void phase, this tends to induce, when the void moves in a dense packing, an “indraght” to the particle located in the active direction. During a sequence of transitions, this void will move a row of grains one at a time but in the same direction. Although the row only moves at a rate of one particle per timestep, a sort of effect of void *propagation* may occur. Let us recall that a phase component is meaningful, only when embedded into the *interaction* law.

4 Modeling a Propagative Mode

4.1 Limitation of the Transition Rule

In spite of the above remark, the transition rule as detailed in Sect. 2.2 is unable to move two contiguous grains when one sends a request to the site of the other.

To illustrate this deficiency, let us consider the scenario in Fig. 3 (for simplicity, an isolated system is assumed). At state t of a one-dimensional system, $m + 1$ solid particles lie in sites denoted here $x, x - 1, \dots, x - m$ while a void lies in site $x + 1$. A downward request is sent by sites $x, x - 1, \dots, x - m$ while an upward request is sent by site $x + 1$. An exchange $x \leftrightarrow x + 1$ is then activated while the m grains above stay at rest. So a void has been inserted in site x , for state $t + 1$, although all grains above have emitted a downward request (case (a)). This elementary transition rule does not allow the void to *propagate* and the grains to tumble down *simultaneously* (as in case (b)).

The question of propagating the void (or more generally the fluid phase) implies that the transition rule be reconsidered. This problem has been dealt with for automata models applied to gravity flows, but the sequential nature of the approach which processes particles from bottom to top violates the principle of simultaneity and Galilean invariance [3]. The solution proposed hereafter leads to a strictly *synchronous* algorithm.

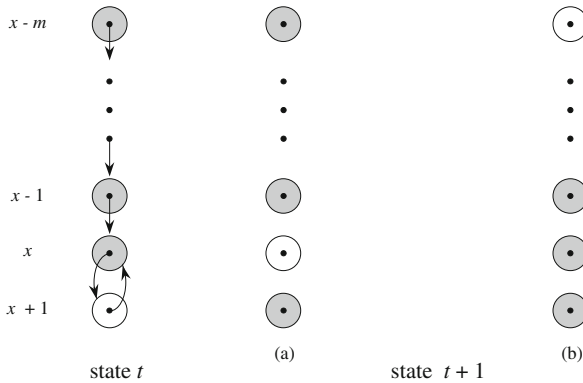


Fig. 3. State t : isolated 1d-system of $m + 1$ solid particles in sites $x, x - 1, \dots, x - m$ acting under gravity; one void in site $x + 1$. State $t + 1$: (a) Elementary (non-propagative) mode: void in site x . (b) Propagative mode: void in site $x - m$.

4.2 Time Evolution: Transition and Timestep

Including a propagative mode leads us to consider transition and timestep at two different scales. In Fig. 3, case (a) represents the outcome of one transition but no longer a state $t + 1$, and case (b) the outcome of $m + 1$ transitions at state $t + 1$ which defines the new timestep. The transition will be said to be *instantaneous* within this timestep.

A first problem is to set up a criterion to stop this transitional sequence, namely a criterion of *termination* for the current timestep. The “physical” principle we adopt is as follows:

- a *grain* is allowed to move at the most one time during a timestep,
- a *void* stayed at rest during a transition remains locked until completion of the current timestep.

It follows that the cell should contain an “activity” signal, to be *disabled* when locking a grain or a void in one of both situations. It is easy to show that this process terminates because the medium is of finite size. Moreover, according to rule R_1 , a void will stop upon reaching the free surface. Consequently, after a finite number of transitions, the scene will no longer contain any active void. Therefore, since only grain-void exchanges are allowed from R_1 , that ensures the end of the current timestep.

A second problem that now arises is to *detect* the termination, a global state which should be perceived at the local scale, namely at the cell level. The detection algorithm runs as follows: at each transition, each cell *broadcasts* over the whole network the binary signal “I have an active void” (true for an active void, false otherwise); conversely, each cell will detect the timestep completion whenever the predicate “There exists one active void!” becomes false; at this time, all the cells will *enable* their activity signal synchronously and initiate the next timestep.

Let us note that this synchronization problem differs from the Myhill-Moore Firing Squad [15,16] because we have no General.

5 Timestep Synchronization

5.1 Systolic Gossiping

The previous action consisting in broadcasting a message from any cell to any other one follows an all-to-all *gossiping* scheme [17]. It should be observed that, in general, gossiping is a more consuming task, in space and time, than broadcasting. For example, given a message of length L and a network of order N , broadcasting requires a buffer of size L whereas gossiping may require a buffer of size NL . But the coarse-grained communications protocols are seldom appropriate for cellular automata. For this reason, further investigations were derived under a “systolic” form (this metaphor was borrowed from H.T. Kung [18]). For fine-grained systolic gossiping, we can refer in particular to [19] and references therein.

For our specific case, this task is much easier to achieve, and this for two reasons: the first one is due to the symmetries of the graph, the second because our buffer is far from exploding. Recall first that our LGrA is constructed on the hexavalent grid, that provides a maximal symmetry for a $2d$ lattice. More precisely, the underlying graph belongs to the family of so-called “rotational” Cayley graphs [20,21] and it is shown therein that this nice property leads to effective gossip schemes. It is beyond the scope of this paper to describe them. Let us just say that there exists a half-duplex 3-port systolic protocol that gossips through the N - SW - SE pattern in a time bounded by $\sqrt{N_s}$ steps [22]. For the

second reason, let us assume the cell having a 1-bit buffer. When receiving the 3-fold signal “There exists one active void!” from its $N-SW-SE$ neighbors, it can immediately reduce it by an “OR” operation. Therefore, a 1-bit buffer suffices to achieve the timestep termination detection.

5.2 The Case Study Revisited

Figure 4 resumes the study of the emptying process with the “3df” law and the same inertial coefficients of Fig. 2c for two different timesteps at $T = 400$ and $T = 1000$ (observe for this state the identical snapshots of Fig. 2c and Fig. 4a). The propagative mode is applied in Fig. 4b. A decrease of porosity appears in this second case as well as the corresponding ebb of the free surface level.

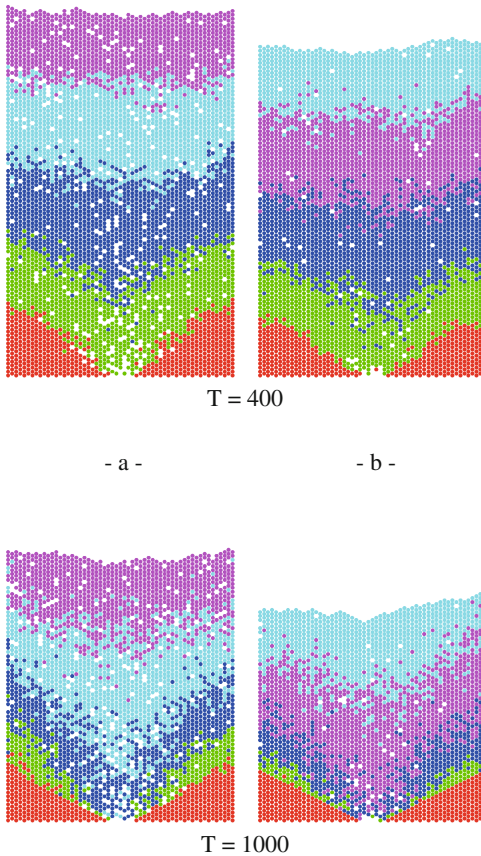


Fig. 4. The “3df” law with rule R_1 governing ϕ_1 and ϕ_2 and inertial coefficients $c_1 = 1$, $c_2 = 10$. States at $T = 400$ and $T = 1000$ (a) without propagative law (b) with propagative law.

Since the snapshots are captured at the end of the timestep, it might seem surprising that all the voids did not reach the free surface. Indeed, if we consider a single void isolated in the bulk, the action of R_1 on both phases implies that a grain-void exchange must occur within the transition and therefore that the void moves up surely. However, it should be pointed out that the grain's site requested by the void is likely to be locked. This means that the void would be about to cross the path of another void that has already spread to the upper layers. Disabling the grain's site caused a lack of response and consequently the retention of the void, which stays at rest. This phenomenon explains how the state of non-zero porosity observed during the silo's emptying process follows from the definition of the criterion of propagation.

Table 1. Impact of the propagative mode on the flow process

$3df \quad H = 101 \quad L = 57 \quad V_0 = 5729 \quad V_0^* = 5391 \quad D = 7$					
	Mode				Ratios
	Non propagative		Propagative		
Timestep	$T = 400$	$T = 1000$	$T = 400$	$T = 1000$	
Voids: N_v	326	240	72	48	
Grains: N_g	4848	3528	4620	2994	
Flow rate Q : $\frac{N_g(t) - N_g(t + \Delta t)}{\Delta t}$	$Q = 2.20$		$Q' = 2.71$		$Q'/Q = 1.23$
Void index: $e = \frac{N_v}{N_g}$	$e = 0.0676$		$e' = 0.0158$		$e'/e = 0.235$
Porosity: $\phi = \frac{e}{1+e}$	$\phi = 0.0633$		$\phi' = 0.0156$		$\phi'/\phi = 0.246$
Relaxation time: $\Delta t_r = \frac{\phi V_0}{Q}$	$\Delta t_r = 165$		$\Delta t'_r = 33$		$\frac{\Delta t'_r}{\Delta t_r} = 0.2$
Discharge time: $\Delta t_v = \frac{V_0^*}{Q}$	$\Delta t_v = 2451$		$\Delta t'_v = 1990$		$\frac{\Delta t'_v}{\Delta t_v} = \frac{Q}{Q'} = 0.81$
Free surface ebb: $U = \frac{H(t + \Delta t) - H(t)}{\Delta t}$	$U = -0.0411$		$U' = -0.0482$		$U'/U = 1.17$
Void mean speed: $u = \frac{H}{\Delta t_r}$	$u = 0.6121$		$u' = 3.075$		$u'/u = 5.02$

The impact of the propagative mode on the flow process in Fig. 4 is analyzed in Tab. 1. V_0^* denotes the dynamical volume of a ‘‘hopper’’ induced by the $3df$ law and out of which a granular dead zone of $V_0 - V_0^* = 338$ cells will stay at rest on both sides of the outlet in the bottom corners of the container. The flow rate remains constant on average from the beginning to the end of the emptying process. As soon as the outlet is opened, the process enters a transient state during a relaxation time before the porosity reaches a maximal threshold and

until the first voids emerge from the free surface. Then the process enters a steady state and the descent of the free surface is activated with constant velocity until completion of a mass flow discharge; note that the “mass flow” pattern is only a consequence of inertial coefficient c_2 . The ratios of the macroscopic quantities between propagative and non propagative modes are given, respectively for flow rate, void index, porosity, relaxation and total discharge times, velocity of the descent of the free surface and vertical mean speed of the void.

6 Conclusion

This paper dealt with the various logical problems induced by the simulation of the physical phenomenon of void propagation in a lattice-grain automata, illustrated with a case study of a silo emptying process. After a short presentation of the transition rule underlying the time evolution in our LGrA, the logic of an inertial memory effect was tackled as well as its influence on the diversity of resulting flow patterns. This background introduced the core of this study: from a simple “physical” criterion governing the void propagation within the medium, a logical framework is proposed to solve the successive problems of synchronization and intensive communications yielded in the cellular automata by this long-range interaction.

Further issues should be pursued. Firstly, the question of “memory effect” must be tackled from its generic sense and in the context of other alternative memory mechanisms [23]. We let also open the question of consistency of our model with the physical time: the time evolution is the main point and, of course, our physical criterion of termination of the void propagation within a row of grains, the perception of the instantaneous transition as well as the transition-timestep duality should be discussed. More precisely, the property of our model regarding Galilean invariance will be examined elsewhere and Lamport’s paradigm [24] between logical clocks and real-time clocks in a distributed system appears as an appropriate startpoint. Besides, a more detailed explanation about the physical results in Tab. 1 will be examined elsewhere [25].

References

1. Chopard, B., Droz, M.: Cellular automata modeling of physical systems. Cambridge University Press, Cambridge (1998)
2. Baxter, G.W., Behringer, R.P.: Cellular automata models of granular flow. *Phys. Rev. A* 42, 1017–1020 (1990)
3. Fitt, A.D., Wilmott, P.: Cellular-automaton model for segregation of two-species granular flow. *Phys. Rev. A* 45(4), 2383–2388 (1992)
4. Peng, G., Herrmann, H.J.: Density waves of granular flow in a pipe using lattice-gas automata. *Phys. Rev. E* 49, R1796–1799 (1994)
5. Károlyi, A., Kertész, J., Havlin, S., Makse, H.A., Stanley, H.E.: Filling a silo with a mixture of grains: friction-induced segregation. *Europhys. Lett.* 44(3), 386–392 (1998)

6. Ktitarev, D.V., Wolf, D.E.: Stratification of granular matter in a rotating drum: cellular automaton modelling. *Granular Matter* 1, 141–144 (1998)
7. Désérable, D., Masson, S., Martinez, J.: Influence of exclusion rules on flow patterns in a lattice-grain model. In: Kishino, Y. (ed.) *Powders and Grains 2001*, Balkema, pp. 421–424 (2001)
8. Cisar, S.E., Ottino, J.M., Lueptow, R.M.: Geometric effects of mixing in 2D granular tumblers using discrete models. *AIChE Journal* 53(5), 1151–1158 (2007)
9. Désérable, D., Dupont, P., Hellou, M., Kamali-Bernard, S.: Cellular automata in complex matter. *Complex Systems* 20(1), 67–91 (2011)
10. Désérable, D.: A versatile two-dimensional cellular automata network for granular flow. *SIAM J. Applied Math.* 62(4), 1414–1436 (2002)
11. Cotteceau, G., Désérable, D.: Open Environment for 2d Lattice-Grain CA. In: Bandini, S., Manzoni, S., Umeo, H., Vizzari, G. (eds.) *ACRI 2010. LNCS*, vol. 6350, pp. 12–23. Springer, Heidelberg (2010)
12. Litwiniszyn, J.: Application of the equation of stochastic processes to mechanics of loose bodies. *Archivum Mechaniki Stosowanej* 8(4), 393–411 (1956)
13. Müllins, W.W.: Stochastic theory of particle flow under gravity. *J. Appl. Phys.* 43, 665–678 (1972)
14. Sakagushi, H., Ozaki, E., Igarashi, T.: Plugging of the flow of granular materials during the discharge from a silo. *Int. J. Mod. Phys.* 7(9,10), 1949–1963 (1993)
15. Moore, E.F.: The firing squad synchronization problem. In: Moore, E.F. (ed.) *Sequential Machines, Selected Papers*, pp. 213–214. Addison-Wesley, Reading (1964)
16. Umeo, H.: Firing squad synchronization problem in cellular automata. *Encyclopedia of Complexity and Systems Science*, 3537–3574 (2009)
17. Liestman, A.L., Richards, D.: Perpetual gossiping. *Parallel Processing Letters* 3(4), 347–355 (1993)
18. Kung, H.T., Leiserson, C.E.: Systolic arrays for VLSI. In: Mead, Conway (eds.) *Introduction to VLSI systems*, pp. 271–292. Addison-Wesley, Reading (1980)
19. Flammini, M., Pérennes, S.: Lower bounds on systolic gossip. *Information and Computation* 196(2), 71–94 (2005)
20. Désérable, D.: A family of Cayley graphs on the hexavalent grid. *Discrete Applied Math.* 93, 169–189 (1999)
21. Heydemann, M.C., Marlin, N., Pérennes, S.: Complete rotations in Cayley graphs. *European Journal of Combinatorics* 22(2), 179–196 (2001)
22. Désérable, D.: Systolic dissemination in the arrowhead (unpublished)
23. Alonso-Sanz, R., Martin, M.: Elementary cellular automata with memory. *Complex Systems* 14(2), 99–126 (2003)
24. Lamport, L.: Time, clocks, and the ordering of events in a distributed system. *Comm. ACM* 21(7), 558–565 (1978)
25. Désérable, D., Lominé, F., Dupont, P., Hellou, M.: Propagative mode in a lattice-grain CA: time evolution and Galilean invariance (to be submitted to) *Granular Matter*